APPENDIX I: EQUILIBRIUM RELATION

Calculation of the enhancement factor ϕ requires a correlation of the equilibrium solubility of CO_2 in aqueous MEA solutions. Of the wealth of data available, almost all are in the form of plots of the equilibrium partial pressure of CO_2 as a function of solution loading with temperature as parameter; this format is quite unsuitable for correlation. When Henry's law is combined with Eq. 20 and the usual exponential dependence on temperature is assumed, the expression

$$p_{CO_2} = Z\left(\frac{\alpha}{1-2\alpha}\right)^2 \exp(-\Delta H/RT) \qquad \text{(A1)}$$

would be most suitable for correlation. Here the parameter Z and the total enthalpy of solution (including reaction) H may depend on concentration and solution loading. The procedure adopted was to fit each set of data in the form $ln\ P_{CO_2}$ vs. α at fixed temperature and MEA concentration with a polynomial of up to third degree in α. This allowed the smoothed data to be converted into the form $ln\ P_{CO_2}$ vs. $1/T$ for fixed α and MEA concentration. Straight lines of the form

$$ln\ p_{CO_2} = A + B\,(10^3/T - 3.0) \qquad \text{(A2)}$$

were fitted through each smoothed data set to obtain the least squares values and standard deviations of A and B. (Data were found to be centered at a temperature of about 60°C; hence, the factor 3.0 appears in Eq. A2 to maintain roughly equal weighting of all data.) Finally, A and B, weighted according to their respective standard deviations, were correlated with solution loading α. For $\alpha < 0.45$ no dependence on MEA concentration was found. The final correlation in the form of Eq. A1 was

$$ln\ p_{CO_2} = -3.70 - 4.83\,\alpha + 2\,ln\,[\alpha/(1-2\alpha)] + (-9.71 - 8.18\,\alpha + 25.2\,\alpha^2)(10^3/T - 3.0) \qquad \text{(A3)}$$

The actual experimental data of Jones et al. (1959), Lawson and Garst (1976), Lee et al. (1974), Lyudkovskaya and Liebush (1949), Mason and Dodge (1936), Mulbauer and Monaghan (1957), Murzin et al. (1969), and Nasir and Mather (1977) are compared with the correlation in Figure A-1. The experimental measurements cover a temperature range from 0°C to 140°C for MEA concentrations between 0.5 N and 9.5 N and solution loadings less than 0.45, and include some 250 points.

The equilibrium data of various workers typically differ from each other by about 50% although differences of a factor of two or three are not uncommon. This is reflected in the considerable scatter which is apparent in Figure A-1. Because of the necessity to go through a preliminary fitting procedure to convert the data into usable form, it cannot be claimed that Eq. A3 is statistically the best fit. However, the procedure adopted does guarantee that the correlation is not unduly biased.

By comparing Eqs. A1 and A3 it can be seen that the total heat of solution is

$$\Delta H = 80.8 + 67.8\,\alpha - 209.0\alpha^2 \qquad \text{(A4)}$$

in MJ/kgmol and that this depends on solvent loading. Danckwerts (1970) reports the heat of solution of CO_2 in water to be about 19.9 MJ/kgmol while Hikita et al. (1977) have found that the heat of reaction of uncarbonated MEA is 75.8 MJ/kgmol at 35°C, and to be temperature dependent. The sum of these two is 95.7 which is about 15% higher than the value 83.7 obtained from Eq. A4 at $\alpha = 0.05$, the smallest value of α in the range correlated.

To calculate the equilibrium constant K all one need do is use Eq. A3 to find p_{CO_2} and relate this to the liquid-phase concentration $[CO_2]_e$ through Henry's law, appropriately modified to account for the presence of all the species in solution.

Laminar Tube Flow with a Thermosetting Polymerization

Two models describing the laminar flow of a polymerizing liquid through a tube have been developed and tested experimentally. One model is a full finite difference solution of the balance equations. The other is an approximate analytical solution which assumes that flow ceases after viscosity increases about tenfold. The models are compared to two experimental cases: 1) the pressure rise needed to keep the flow rate through the tube constant and 2) the flow rate decrease when pressure at the tube entrance is held constant. The finite difference model is more accurate in the early stages of polymerization while the approximate analytical model is more accurate at long times. The models have application to runner flow in reaction injection molding, to nozzles in thermoset molding, to thermoset dispensing equipment and to continuous reactive polymer processes in general.

J. M. CASTRO, S. D. LIPSHITZ and C. W. MACOSKO

Department of Chemical Engineering and Materials Science University of Minnesota Minneapolis, MN 55455

SCOPE

The introduction of Reaction Injection Molding (RIM), (Prepelka and Wharton, 1975; Lee, 1980) has resulted in considerable interest in molding thermosetting polyurethanes. Whereas high pressures are needed to injection mold conventional, high viscosity thermoplastic materials, the low viscosities of the polyurethane reactants allow a mold to be filled using much lower pressures. RIM is thus particularly advantageous in molding large surface area parts and is being used, among

J. M. Castro is presently with the Planta Piloto de Ingeniería. Química, Universidad Nacional del Sur, Bahia Blanca, Argentina; S. D. Lipshitz, IMI Institute for Research and Development, Box 313, Haifa 3100, Israel.

0001-1541-82-8568-0973-$2.00.

other applications, for appliance cabinets and automobile front and rear ends.

The RIM process can be broken down into several stages. These include: component metering; intensive mixing to bring the reactants into intimate molecular contact within a time scale short compared to the process cycle time; flow into the final shape, such as filling a mold; reaction or curing in shape until the part is stiff enough to remove; and post curing, used to improve modulus and dimensional stability.

From the mixing head, before entering the mold, the reactive mixture flows through the runner. The runner flow can be assumed a continuous process, since its average residence time is much smaller than the total filling time. The main difference, with respect to the flow in the mold (batch process), is that the flow front can be neglected. All the flow modelling studies that have been done in RIM (Domine and Gogos, 1980; Kamal and Ryan, 1980; Castro and Macosko, 1982) neglect the runner flow. The goal of this work is to develop and experimentally test a model for it. A cylindrical geometry was chosen and the model set up to work in either of two cases. In the first, it predicts the pressure rise needed to keep the flow rate through the tube constant. In the second it predicts the flow rate decrease if the pressure at the tube entrance is kept constant. Both situations are of practical importance. Constant flow rate will occur if positive displacement pumps are used in RIM equipment. Alternatively, a constant pressure metering device can be used, or a hydraulic device, which would be flow rate limited up to a maximum pressure at which it becomes pressure limited (Lord and Williams, 1975). The model was experimentally tested under both cases.

The model has application beyond RIM, to nozzles in thermoset molding and to continuous reactive polymer processes (Biessenberger and Gogos, 1980) such as foam dispensing equipment, reactive extrusion and reactive coating operations.

CONCLUSIONS AND SIGNIFICANCE

As expected in a tubular reactor with a thermosetting polymerization, pressure continuously increases under constant flow rate conditions or the flow rate decreases under limiting pressure. A model has been developed to predict both the pressure rise with constant flow rate and the flow rate decrease with constant pressure drop through the reactor. The model is general, it is applicable to isothermal and nonisothermal situations. The model requires numerical integration using finite difference techniques of the balance equations. When compared to experiments on a polyurethane system, for the constant flow rate case it predicts fairly well more than one decade of the pressure rise. Higher rates are underpredicted. For the limiting pressure experiments it predicts fairly well the flow rate decrease over the entire range.

An approximate analytical solution is also developed for both cases. The solution assumes that the flow is isothermal, and that flow along a stream line becomes negligible when viscosity rises to $\eta \cong 3\eta_o$. The analytical solution gives better predictions than the numerical simulation in the high pressure region.

MATHEMATICAL MODEL

A mathematical model was developed to describe flow through a tube of a polymerizing mixture. The following assumptions were made:

1) Constant density, heat capacity, thermal conductivity and heat of reaction. These quantities do not vary significantly with polymerization or temperature for thermosetting and elastomeric materials (Van Krevelan, 1978; Lipshitz and Macosko, 1977).

2) Negligible mass and thermal diffusion in the axial direction. The diffusivities are low and L/D values large.

3) n^{th} order kinetics with Arrhenius temperature dependence

$$dC_a/dt = R_a = k(T)C_a^n = k_o e^{-(E/R_g T)}C_a^n \tag{1}$$

The kinetic mechanisms are generally more complex than simple n^{th} order but, for process modelling what we need are only phenomenological equations. These may not necessarily reflect the true kinetics but do a good job in describing the overall chemical reaction (Richter and Macosko, 1978). For the chemical system used in the experiments, a 1.5 order equation fit overall conversion data well as shown by Lipshitz and Macosko (1977).

4) Newtonian fluid, that is, the viscosity is only an explicit function of the extent of reaction and temperature.

$$\eta = \eta(C^*, T) \tag{2}$$

No shear thinning was observed for the materials used, up to at least a 200-fold viscosity increase (Lipshitz and Macosko, 1976).

5) Laminar flow, low Reynolds number.

6) Inertial terms in the momentum equation may be ignored in view of the low Reynolds numbers.

7) Quasisteady state is assumed for the momentum equation; i.e., polymer build up on the tube wall is slow. This assumption also is commonly made in calculations involving heat transfer to flowing thermoplastic polymers (Tadmor et al., 1974, 1975).

8) Neglect entrance length, $L/D \gg 1$.

9) Unidirectional flow (v_r, v_θ negligible with respect to v_z), lubrication approximation (Tadmor and Gogos, 1979).

10) At time zero, the tube is completely filled with unreacted mixture.

Application of the above assumptions reduces the balance equations, in dimensionless variables (defined in the nomenclature section) to the following forms

Momentum balance

$$\frac{\partial v_z^*}{\partial r^*} = \left(\frac{\partial p}{\partial z}\right)^* \frac{4r^*}{\eta^*} \tag{3}$$

Mass balance

$$Q^* = 2\int_0^1 r^* v_z^* dr^* \tag{4}$$

Integration of the mass balance by parts using the no slip boundary condition gives

$$Q^* = -\int_0^1 r^{*2}\left(\frac{\partial v_z^*}{\partial r^*}\right) dr^* \tag{5}$$

Substituting Eq. 3 in Eq. 5 yields

$$Q^* = -4\left(\frac{\partial p}{\partial z}\right)^* \int_0^1 \frac{r^{*3}}{\eta^*} dr^* \tag{6}$$

Integrating Eq. 3 and combining it with Eq. 6 gives

$$v_z^* = \frac{Q^* \int_{r^*}^1 \frac{r^*}{\eta^*} dr^*}{\int_0^1 \frac{r^{*3}}{\eta^*} dr^*} \tag{7}$$

The total pressure drop through the tube can be obtained integrating Equation (6) all the way from the tube entrance to the exit to obtain

$$\Delta p^* = \frac{Q^*}{4} \int_0^1 \frac{dz^*}{\int_0^1 \frac{r^{*3}}{\eta^*} dr^*} \tag{8}$$

With the assumptions given above the mole balance becomes

$$\frac{\partial C^*}{\partial t^*} + v_z^* \frac{\partial C^*}{\partial z^*} = Gk^*(1 - C^*)^n + \frac{1}{\mathrm{Pe}_m} \frac{1}{r^*} \frac{\partial}{\partial r^*} \left(r^* \frac{\partial C^*}{\partial r^*} \right) \tag{9}$$

where G and Pe_m are the gelling potential (Castro and Macosko, 1982) and the Peclet number for mass transfer respectively. They are defined as

$$G = \frac{\text{initial residence time}}{\text{isothermal gel time at } T_o} = \frac{t_{r_o}}{t_{g_o}} \tag{10}$$

$$\text{and } \mathrm{Pe}_m = \frac{\text{mass transport by convection}}{\text{mass transport by diffusion}} = \frac{(\bar{v}_z/L)C_o}{(D_{AB}/R_o^2)C_o}$$

$$\text{or} = \frac{\text{characteristic mass diffusion time}}{\text{initial residence time}} = \frac{R_o^2/D_{AB}}{t_{r_o}} \tag{11}$$

The balance of energy reduces to

$$\frac{\partial T^*}{\partial t^*} + v_z^* \frac{\partial T^*}{\partial z^*} = Gk^*(1 - C^*)^n + \frac{1}{\mathrm{Pe}} \frac{1}{r^*} \frac{\partial}{\partial r^*} \left(r^* \frac{\partial T^*}{\partial r^*} \right) + \frac{Br}{\mathrm{Pe}} \eta^* \left(\frac{\partial v_z^*}{\partial r^*} \right)^2 \tag{12}$$

where the Peclet and Brinkman number are defined as

$$\mathrm{Pe} = \frac{\text{heat transport by convection}}{\text{heat transport by conduction}} = \frac{(\bar{v}_z/L)\rho C_p \Delta T_{ad}}{(\hat{k}/R_o^2)\Delta T_{ad}} = \frac{R_o^2 \rho C_p/\hat{k}}{t_{r_o}} \tag{13}$$

$$Br = \frac{\text{heat production by viscous dissipation}}{\text{heat transport by conduction}} = \frac{\eta_o(\bar{v}_z/R_o^2)}{(\hat{k}/R_0^2)\Delta T_{ad}} \tag{14}$$

Equations 7, 8, 9 and 12 were integrated numerically using finite difference techniques, note that they are coupled since the viscosity is a function of extent of reaction and temperature. Since the viscosities in these systems are typically low, $Br \ll 1$ and viscous dissipation effects can be neglected. The following initial and boundary conditions were used

Initial conditions

$$t = 0 \qquad C^* = 0$$

$$T^* = 0$$

$$Q^* = 1$$

Boundary conditions

$z = 0$	$T^* = 0$	$C^* = 0$
$r = 0$	$(\partial T^*/\partial r^*) = 0,$	$(\partial C^*/\partial r^*) = 0$
$r = R$	$T^* = 0,$	$(\partial C^*/\partial r^*) = 0$

NUMERICAL SOLUTION

In order to commence an integration step between t and $t + \Delta t$, C^* and T^* must be defined. η can then be calculated from data on the chemical reactants (Lipshitz, 1976). The instantaneous velocity profiles v_z are calculated from Eqs. 7 and 8. v_z is assumed to remain constant during the period t and $t + \Delta t$. If the flow rate is constant, Eq. 7 is integrated directly. When Δp is specified, the instantaneous flow rate is obtained from Eq. 8 and substituted in Eq. 7 to obtain the velocity profiles. Once v_z is known Eqs. 9 and 12 can be integrated over the interval t to $t + \Delta t$.

To reduce computation time, explicit rather than implicit methods were used to integrate Eqs. 9 and 12. These are generally faster, but some sacrifice is made in accuracy and stability (Carnahan et al., 1969). In addition, Eqs. 9 and 12 were uncoupled for the integration interval, Δt, by using $T^*(t)$ in integrating Eq. 9 and $C^*(t)$ in Eq. 12. A forward difference was used for the time derivative, a backward difference for the convective term and Saul' yev's explicit; alternating direction method (Carnahan et al., 1969) for the diffusion terms. Equations 7 and 8 were integrated using Simpson's rule.

TABLE 1. GRAETZ PROBLEM: COMPARISON OF THEORETICAL EXIT TEMPERATURE TO NUMERICAL RESULT

$T_{\text{inlet}} = 338$ K, Pe = 1.64, Theoretical	$T_{\text{wall}} = 318$ K, $Q = 10$ cm^3/min, 9 × 9 grid	15 × 11 grid	17 × 13 grid
319.760 K	319.944 K	319.848 K	319.833 K

A grid of 17 radial and 13 axial increments was used for most calculations. Numerical instability originated in the convective term. Stability was found to be assured for

$$v_z^* \frac{\Delta t^*}{\Delta z^*} < 1$$

Kamal and Kenig (1972) report the same stability limitation in simulating thermoplastic injection molding.

Equally spaced increments were taken in the axial direction. Ideally we would like smaller radial increments in the region where the concentration and velocity gradients are largest. However this region moves inward with time, as will be discussed later. Consequently, it was not useful to concentrate the grid at any single radial location.

The program was written in Fortran IV and run on a CDC-6600 computer. Computation time varied from 80 to 140 seconds for simulating a constant flow rate experiment, and from 25 to 50 seconds for a limited pressure experiment.

To test the program, two simpler steady state cases to which theoretical solutions exist, were simulated. Typical flow conditions were used: (10 cm^3/min flowing through a 3.5 mm diameter tube 650 mm long with T_w at 318 K).

Case A. Fully developed flow of a Newtonian fluid with uniform physical properties through a heated and cooled tube (the Graetz problem, see McAdams, 1954).

The parabolic velocity profile and reduced pressure drop of unity are simulated to better than 6 significant figures. The theoretical cup-averaged exit temperature is compared to numerical results in Table 1, for a tube wall 20 K lower than the inlet temperature.

Case B. An isothermal reactor with parabolic velocity profiles. Each fluid element behaves like a batch reactor, with reaction time equal to the residence time of the element. Table 2 compares theoretical and numerical results, for various residence times. Agreement for conversion is within 2% (Lipshitz, 1976).

EXPERIMENTAL CONDITIONS

A two component thermosetting polyurethane system, an extended diisocyanate prepolymer of 1,6 hexamethylene diisocyanate (18.5% NCO) and a ϵ-caprolactone based triol, were used. These materials have been

TABLE 2. EXTENT OF REACTION IN AN ISOTHERMAL REACTOR WITH CONSTANT VISCOSITY AND NO DIFFUSION. THEORETICAL AND NUMERICAL RESULTS WITH KINETICS OF EQ. 15

Residence Time (min)	Extent of Reaction, C^*: Theoretical	Numerical 13 Axial Grid Points	Numerical 21 Axial Grid Points
0.725	0.2335	0.2273	0.2297
1.087	0.3208	0.3150	0.3172
1.265	0.3582	0.3512	0.3539
1.45	0.3939	0.3856	0.3887
1.78	0.4514	0.4409	0.4449
2.48	0.5482	0.5338	0.5393
4.64	0.7259	0.7050	0.7112

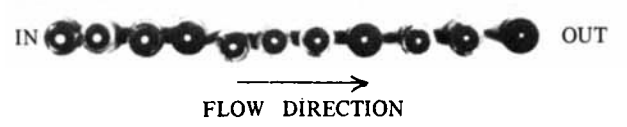

Figure 1. Reactor cross sections after experiment 3Q, t = 4.72 min, flow rate Q_o = 10 cm³/min.

described in detail by Lipshitz and Macosko (1976, 1977).

An experimental apparatus was built to preheat the two components, meter them in the correct ratio, mix them and flow the mixture into a tubular reactor. The brass reactor, 648 mm long, 4.7 to 1.9 mm internal diameter, was held in a constant temperature water bath at 318 K ± 0.3 K. The apparatus and procedure have been described in detail by Lipshitz (1976).

Two types of experiments were conducted, constant flow rate and limiting pressure. When the flow rate was held constant, the pressure was observed to rise continuously. When pressure reached 690 kPa, the low viscosity material was flushed from the reactor by dispensing only the triol component. Sectioning the reactor revealed a gelled layer deposited on the walls and a polymer free central core. A photograph of such sections is shown in Figure 1. For the limiting pressure experiments, initially the flow rate was kept constant until the limiting pressure of 20.7 kPa was reached, from then on the pressure was kept constant by manually reducing the piston pump speed. Experiments were terminated when the flow rate fell below 0.5 cm³/min. When the initial pressure rise of these experiments was compared to the previous constant flow rate experiments it was found that the time to reach 20.7 kPa was uniformly longer. Thus the limiting pressure experiments were all shifted 1 minute. The individual experiments are summarized in Table 3.

KINETICS, THERMAL AND PHYSICAL PROPERTIES

To solve the balance equations we need to know the thermal, kinetic and rheological properties of the reactive system. Detailed information on the acquisition of the thermal and kinetic data is given by Lipshitz and Macosko (1976, 1977). Reaction kinetics were described by

$$\frac{dC_a^*}{dt} = 3.14 \times 10^8 e^{-(64640/R_gT)} C_o^{0.5}(1 - C^*)^{1.5} \frac{\text{g-equiv}}{\text{m}^3\cdot\text{min}} \tag{15}$$

The initial reactive group concentration (C_o) was 2.64×10^3 g-equiv/m³. Note that the numerical value for k_o given by Lipshitz and Macosko (1977) in their eq. 8 is a misprint, corrected here.

Heat capacity of 1875 J/kg·K and thermal conductivity of 0.188 W/m·K were measured for the solid polymer at 313 K. Heat of reaction is 60.33 kJ/g-equiv. A density of 1.075 g/cm³ was used. This is an average value for the two liquid reactants. Density at complete reaction was 1.135 g/cm³.

The following equation was found to give a good fit to the viscosity data (Lipshitz and Macosko, 1976).

$$\eta = 4.747 \times 10^{-8} \exp\frac{41650}{R_gT}\left[\frac{\overline{M}_w}{\overline{M}_{w_o}}\right]^{(20960/R_gT\ -\ 5.3176)} \tag{16}$$

where η is in Pa·s, $\overline{M}_{w_o}$ = 796 and R_g = 8.3192 J/g·mol·K. M_w is related to the extent of reaction C* by Eq. 8 of Lipshitz and Macosko (1976). For the system used here $\overline{M}_{n_1}$ = 454, $\overline{M}_{w_1}$ = 810, $\overline{M}_{n_2}$ = 537 and $\overline{M}_{w_2}$ = 715 thus

$$\overline{M}_w = 768 + C^*\left[\frac{1725\,C^* + 1200}{1 - 2\,C^{*2}}\right] \tag{17}$$

Mass diffusion coefficients are expected to be low because of the high viscosities involved. If mass diffusion were significant, high viscosity material could move from the walls to the tube center, and be removed. At high shear rates, a scouring mechanism might remove gelled polymer. For constant flow rate, a steady state would be achieved if radial mass transfer or scouring were significant. No steady states were, however, observed for the experimental constant flow rate range covered. Even for the smallest diameter tube (1.9 mm), in which diffusion effects would be greatest, the pressure was observed to rise continuously to the limit of 690 kN/m². These experimental observations indicate mass diffusion is indeed negligible.

TABLE 3. EXPERIMENTAL CONDITIONS

Experiment	Reactor Length = 64.8 cm, t_{g_o} = 4.3 min: 1Q, 1P	2Q, 2P	3Q, 3P	4Q, 4P	5Q
Radius, R_o (cm)	0.236	0.175	0.236	0.175	0.095
Flow Rate, Q_o (cm³/min)	5.22	5.22	10.00	10.00	5.22
Initial Res. Time (s)	130.5	72.0	70.2	37.2	21.0
Re	0.038	0.052	0.074	0.099	0.095
G	0.506	0.279	0.272	0.144	0.082
Pe_m	4270	4250	7930	8230	4300
Pe	0.48	0.48	0.91	0.91	0.48
Br	1×10^{-6}	2×10^{-6}	2×10^{-6}	1×10^{-6}	7×10^{-6}

Note that Q refers to constant flow rate, and P to limiting pressure experiment.

Wallis et al. (1975) found mass diffusion to be negligible. Broyer and Macosko (1976) ignored mass diffusion in modeling static curing of a thermoset. They estimated $D_{AB} = 10^{-9}$ cm²/s. Sala et al. (1974) used $D_{AB} = 10^{-8}$ cm²/s in modeling a polystyrene tubular reactor. Simulations run in the present study showed $D_{AB} = 10^{-8}$ cm²/s had an insignificant effect on results for the 1.9 mm diameter tube. Lynn and Huff (1971) used $D_{AB} = 10^{-5}$ cm²/s (for ethanol diffusing through water, $D_{AB} = 1.28 \times 10^{-5}$ cm²/s) and found an insignificant effect on their results. Their smallest tube diameter was 19 mm. Simulations for the largest tube diameter used in this study, 4.7 mm, were similarly unaffected by $D_{AB} = 10^{-5}$ cm²/s. Simulation of the 1.9 mm tube, however, did show an effect (Lipshitz, 1976).

In view of the fact that no steady states were observed experimentally and that the smallest tube diameter was sensitive only to an unrealistically high D_{AB}, the diffusion term was omitted from all further simulations.

RESULTS

The pressure increase with time recorded during constant flow rate experiments is shown in Figures 2 to 4. Each experiment was repeated at least twice. There is a general trend present in all the

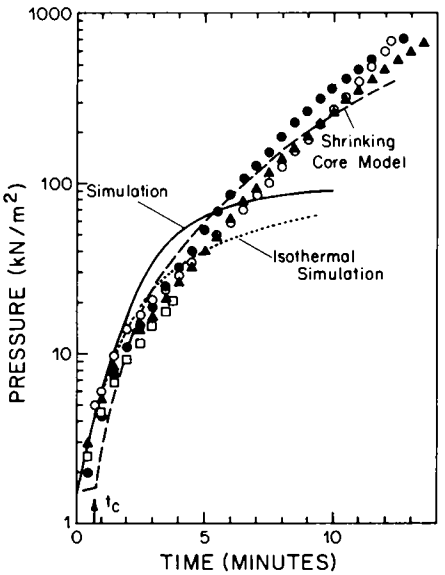

Figure 2. Pressure drop over reactor as a function of time for constant flow rate experiment 1Q. Symbols are experimental results (three repeated runs). Solid line full nonisothermal, finite difference simulation, dotted line isothermal simulation, dashed line approximate analytical solution (Appendix).

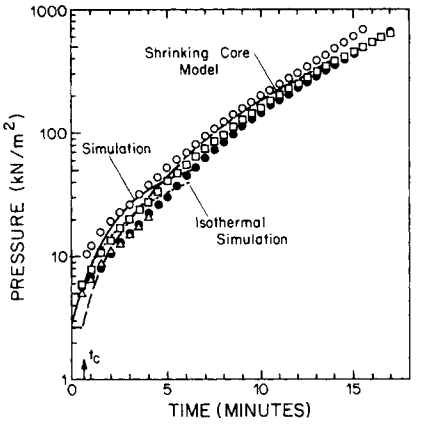

Figure 3. Pressure drop over reactor as a function of time for constant flow rate experiment 3Q. Symbols are experimental results. Lines same as Figure 2.

results: Pressure increase is initially very rapid. After three or four minutes it decreases to a fairly steady exponential rise. Computer simulated results of the constant flow rate experiments are shown in the Figures. Both isothermal and nonisothermal solutions are similar indicating that temperature effects are not large for these small diameter tubes. The fast initial pressure rise is predicted fairly well. Beyond three to five minutes, the pressure drop is considerably underestimated. Note that the isothermal gel point of the polymerization is 1.63 minutes at 318 K. In actual equipment it would be unusual to permit more than a tenfold increase in pressure. The simulation is adequate over this range.

Figures 5 and 6 give the results of the limiting pressure experiments. In each case when the maximum pressure of 20.7 kPa is reached the flow rate decays rapidly. With decreasing initial flow rate (increased residence time) the time for the tube to block up decreases as the asymptotic decrease in Q indicates. Numerical simulations of the limiting pressure experiments are fairly good. They are shown as solid lines in Figures 5 and 6.

DISCUSSION

In all the experiments, the tube is initially filled with an unreacted mixture. The initial pressure rise is due to reaction and viscosity increase of the entire tube contents. As time proceeds, since the material adjacent to the wall has a prolonged residence time, considerable reaction and viscosity increase occurs there. This high viscosity material will flow still slower and on further reaction will effectively cease flowing. This material acts like the tube wall, retarding the velocity of the adjacent material. The phenomena

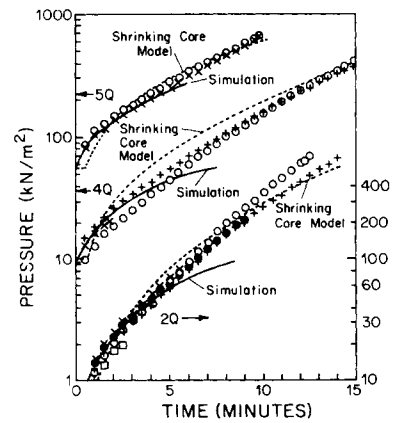

Figure 4. Pressure drop over reactor as a function of time for constant flow rate experiments 2Q, 4Q and 5Q. Lines same as Figure 2.

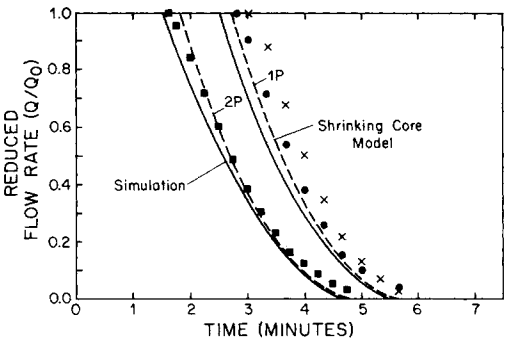

Figure 5. Flow rate decay with time for limiting pressure experiments 1P and 2P.

is continuous, causing the effective tube diameter to steadily contract. This becomes clear by looking at Figure 7 which shows the simulated variation of velocity profiles during constant flow rate for experiment 2Q at $z' = 0.5$.

After a period of time, a wall build up similar to that shown experimentally in Figure 1 and schematically in Figure 9 will be reached. This has the effect of moving inward the region where the gradients are the sharpest, as can be seen for the velocity and conversion in Figures 7 and 8 respectively. Since the residence time in the central core is low, conversion will be low. The majority of the pressure drop observed is simply due to the flow of unreacted material in an ever decreasing central core. The error in the high pressure region may be due to the inability of the finite difference method to accurately model the ever decreasing duct. As the solid layer builds up on the tube wall the number of grid points in the flow cross section decreases. This means fewer difference points are available to describe the ever increasing gradients in the viscous layer. This problem is also encountered when modelling the freezing of flowing systems. A radial grid which moves inward with wall buildup is needed. Such work is in progress.

One approach to predicting the high pressure region with greater accuracy is to model the wall layer build up directly. Such a "shrinking core model" is developed in the Appendix. It requires isothermal flow and estimation of a critical time t_c at which flow effectively ceases. With a single t_c value all the results are fit fairly well as indicated by the dashed lines in Figures 2 to 6.

ACKNOWLEDGMENT

This work was supported by grants from the Union Carbide Corp. and the National Science Foundation, Div. of Materials Research, Polymer Program and Industry University Cooperative Research Program.

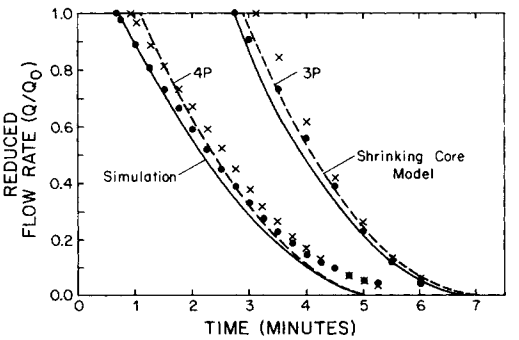

Figure 6. Flow rate decay with time for limiting pressure experiments 3P and 4P.

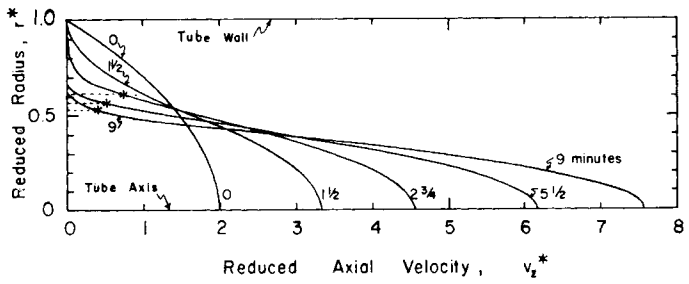

Figure 7. Simulated variation of velocity profiles with time during constant flow rate experiment 2Q at $z^* = 0.5$.

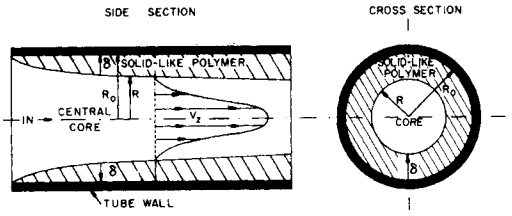

Figure 9. Representation of laminar tubular polymerization reactor. From $r = 0$ to R-δ is the central core where practically all flow occurs. From $r = R$-δ to R_o is a layer of polymer that is essentially solid. R decreases with time due to the polymerization.

APPENDIX

Shrinking Core Model

The viscosity rise of many thermoset systems can be roughly approximated by a step function. That is, the material can be assumed to remain at its initial viscosity, until some critical extent of reaction at which the viscosity suddenly becomes infinite. Another way to view this is that after some critical flow time t_c along a stream line viscosity has increased such that the flow effectively stops. With this approximation and assuming that the flow is isothermal, an analytical solution can be obtained for the constant flow rate experiments. The solution for the limiting pressure experiments, using this approach, requires only a simple numerical integration.

Assuming that the flow is isothermal as discussed before is valid in our case due to the small tube diameters. The true flow, can then be approximated as the flow of a Newtonian fluid with constant viscosity η_o, through a tube of slowly decreasing diameter (central core). These ideas are used below to develop a model, based in predicting the tube diameter shrinkage.

Core Radius

A material particle flowing at a distance δ from the reactor wall ($\delta \ll R$, note Figure 9) will be at a position z in a time t given by

$$t = \frac{z}{v_z(\delta)} \tag{A1}$$

If t equals the time needed for the viscosity to become infinite, t_c, the particle stops flowing. Thus at time t_c all particles with a velocity smaller or equal to

$$v_z(\delta) = \frac{z}{t_c} \tag{A2}$$

stop flowing. Expanding v_z in a Taylor series around $r = R$ we get

$$v_z(\delta) = v_z(R) - (\partial v_z/\partial r)_{r=R}\,\delta + 0(|\delta|)^2 \tag{A3}$$

since $\delta \ll 1$ and $v_z(R) = 0$, we get

$$v_z(\delta) \approx -(\partial v_z/\partial r)_{r=R}\delta \tag{A4}$$

Combining Eqs. A2 and A4, we can obtain an expression for the layer (δ) deposited at time t_c.

$$\delta = -z/t_c(\partial v_z/\partial r)_{r=R} \tag{A5}$$

For times longer than t_c, the core radius will shrink in a continuous fashion. Since, a polymer layer of thickness δ is deposited in time t_c, it seems appropriate to assume that:

$$\frac{-dR}{dt} = \frac{\delta}{t_c} \tag{A6}$$

Note that δ is not constant; it decreases with time since $(\partial v_z/\partial r)_{r=R}$ increases as the core diameter shrinks.

Substituting Eq. A5 for δ into Eq. A6 and $(\partial v_z/\partial r)_{r=R}$ from the integration of the balance of linear momentum with constant viscosity η_o, we obtain

$$\frac{dR}{dt} = \frac{2z\eta_o}{t_c^2 R\,\dfrac{\partial p}{\partial z}} \tag{A7}$$

Substituting for $\partial p/\partial z$ in terms of the flow rate the differential equation describing the core shrinkage becomes

$$\frac{-dR}{dt} = \frac{zR^3\pi}{4t_c^2 Q} \tag{A8}$$

For the constant flow rate case Eq. A8 can be integrated directly with the initial conditions that $R = R_o$ at $t = t_c$, to obtain

$$R = R_o\left\{\frac{1}{1 + \dfrac{z\pi R_o^2}{2t_o^2 Q}(t - t_c)}\right\}^{1/2} \tag{A9}$$

Figures 10 and 11 compare the predictions of Eq. A9 using t_c = 40 seconds with experimental results. Note that at 318 K in 40 seconds $C^* = 0.219$ (eq. 15) which corresponds to $\eta = 0.85$ Pa·s (eq. 16). Figure 10 shows the reduced core diameter (R/R_o) as a function of time midway between the reactor entrance and exit for experiment 2Q. Figure 11 shows the predicted core diameter as a function of axial position for two different times also for experiment 2Q. The experimental results were obtained by flushing the reactor at the desired time with only one of the reactants; after which, the reactor was sectioned as shown in Figure 1 and the core

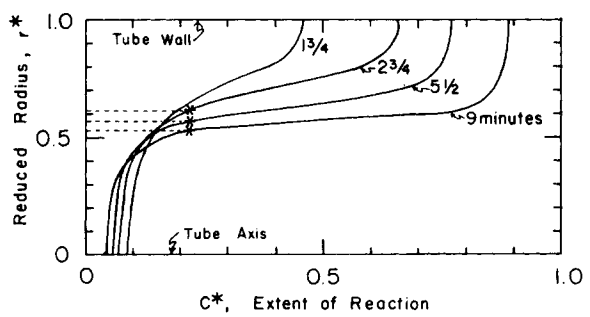

Figure 8. Simulated variation of extent of reaction profiles during constant flow rate experiment 2Q at $z^* = 0.5$.

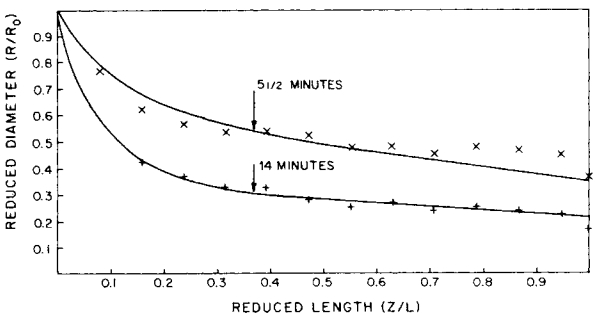

Figure 10. Comparison of experimental (2Q) to predicted (eq. A9) core diameter variation with time, at $z^* = 0.5$.

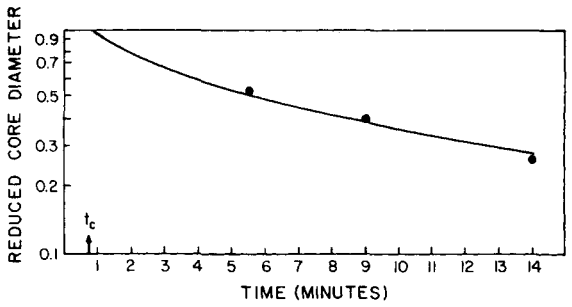

Figure 11. Comparison of experimental to predicted core diameter profiles with time in a constant flow rate experiment.

diameter measured. As can be seen the predictions of Eq. A9 agree closely with the experimental results.

The pressure gradient is obtained by substituting the core radius expression A9 into the integrated balance of linear momentum, to obtain

$$\frac{-\partial p}{\partial z} = \frac{8\eta_o Q}{\pi R_o^4}\left\{1 + \frac{z\pi R_o^2}{2t_c^2 Q}(t - t_c)\right\}^2 \tag{A10}$$

The pressure drop through the reactor is then

$$\Delta p = \int_0^L \frac{\partial p}{\partial z}\, dz \tag{A11}$$

Substituting Eq. A10 into Eq. A11 we get

$$\Delta p = \frac{8Q\eta_o}{\pi R_o^4}\left\{L + \frac{\pi R_o^2(t - t_c)}{2t_c^2 Q}L^2 + \left[\frac{\pi R_o^2(t - t_c)}{2t_c^2 Q}\right]^2 \frac{L^3}{3}\right\} \tag{A12}$$

The predictions of Eq. A12 using $t_c = 40$ seconds are shown as the dashed lines in Figures 2–4. Note that the pressure drop remains constant up to t_c, which is a consequence of assuming that the viscosity rise is a step function.

When the flow rate is not constant, the integration of Eq. A8 gives

$$R = R_1\left\{\frac{1}{\dfrac{1 + 2\pi R_1^2 z}{4t_c^2}\displaystyle\int_{t_1}^{t}\frac{dt}{Q}}\right\}^{1/2} \tag{A13}$$

where R_1 is the core radius at the time when the constant pressure drop regime begins (t_1) and is obtained using Eq. A9.

The flow rate as a function of time is given by

$$Q = \frac{\Delta p \pi}{8\eta_o \displaystyle\int_0^L \frac{dz}{R^4}} \tag{A14}$$

where Δp is the value of the limiting pressure.

Substituting Eq. A13 into Eq. A14 and integrating we obtain

$$Q = \frac{\Delta p \pi R_o^4}{8\eta_o}\left\{\frac{1}{L + eL^2 + e^2\dfrac{L^3}{3}}\right\} \tag{A15}$$

where

$$e \equiv a + R_o^2 f(t) b$$
$$a \equiv (\pi R_o^2/2t_c^2 Q_o)(t_1 - t_c)$$
$$b \equiv (\pi/2t_c^2)$$
$$f(t) \equiv \int_{t_1}^{t}\frac{dt}{Q}$$

To solve Eq. A15, the flow rate is assumed to remain constant for a period Δt. Thus we calculate $f(t + \Delta t)$ using $Q(t)$ and then use $f(t + \Delta t)$ to calculate $Q(t + \Delta t)$. The predictions of Eq. 15 are shown as dashed lines in Figures 5 and 6.

As can be seen the shrinking core model does a good job in predicting both types of experiments. Furthermore, it gives a simple equation to predict the tube diameter shrinkage. It requires isothermal flow and the estimation of a critical time at which flow becomes negligible. However with a single t_c value all the results are fit fairly well. To establish t_c for a different chemical system, one could run a tube plugging experiment similar to the one used to obtain Figure 11 and use the value which best fits the data to Eq. A9. A rule of thumb may be $t = t_c$ when $\eta \approx 3\,\eta_o$.

NOTATION

C = concentration of reactive species at time t
C_o = initial concentration of reactive species = 2.64×10^3 g-equiv/m^3
C^* = extent of reaction: $(C_o - C)/C_o$
C_g^* = gel point = 0.707
C_p = heat capacity at constant pressure = 1875 J/kg·K
D_{AB} = diffusion coefficient $< 10^{-5}$ cm^2/s
E = activation energy = 64.64 kJ/g·mol
H_r = heat of reaction = 60.33 kJ/g equiv.
k = thermal conductivity = 0.188 W/m·K
k_o = pre-exponential factor in kinetic constant
k = kinetic rate constant
k_{T_o} = kinetic rate constant evaluation at T_o
k^* = dimensionless reaction rate:

$$\frac{k}{k_{T_o}(n-1)}\left\{\frac{1 - (1 - C_g^*)^{n-1}}{(1 - C_g^*)^{n-1}}\right\}$$

L = reactor length
$\overline{M}_w$ = weight average molecular weight
$\overline{M}_{w_o}$ = initial weight average molecular weight = 796
n = reaction order = 1.5
p = pressure
Q = flow rate
Q_o = initial flow rate (limiting pressure experiments)
Q^* = dimensionless flow rate: Q/Q_o
R = central core radius
R_g = gas constant
R_o = reactor radius
r = radial variable
r^* = dimensionless radius = r/R_o
T = temperature
T_o = initial temperature (wall temperature)
T^* = dimensionless temperature: $T - T_o/\Delta T_{ad}$
t = time
t_c = time for viscosity to rise sufficiently that flow effectively stops
t_{r_o} = initial residence time = $L/\bar{v}_z$
t_{g_o} = time to reach gel point at T_o:

$$\frac{1}{(n-1)kC_o^{n-1}}\left[\frac{1 - (1 - C_g^*)^{n-1}}{(1 - C_g^*)^{n-1}}\right]$$

t^* = dimensionless time: t/t_{r_o}
v_z = axial velocity
v_z^* = dimensionless velocity: $v_z/\bar{v}_z$
$\bar{v}_z$ = average velocity = $Q/\eta R_o^2$
z = axial variable
z^* = dimensionless axial variable
$\left(\dfrac{\partial p}{\partial z}\right)^*$ = dimensionless pressure gradient = $(\partial p/\partial z)/(8\eta_o Q/\pi R_o^4)$

Greek Symbols

α = thermal conductivity = $k/\rho C_p$
η = viscosity
η_o = viscosity evaluated at $T = T_o$ and $C = C_o$
η^* = dimensionless viscosity: η/η_o
ρ = density

ΔT_{ad} = adiabatic temperature rise: $\frac{H_r C_o}{\rho C_p}$

Δp = pressure drop over reactor length

Δp_o = initial pressure drop = $\frac{8Q\eta_o L}{\pi R_o^4}$

Δp^* = dimensionless pressure drop: $\Delta p / \Delta p_o$

LITERATURE CITED

Biessenberger, J. A., and C. G. Gogos, "Reactive polymer processing," *Polym. Eng. Sci.*, **20**, 13, 838 (1980).

Broyer, E., and C. W. Macosko, "Heat transfer and curing in polymer reaction molding," *AIChE J.*, **22**, 268 (1976).

Carnahan, B., N. A. Luther, and J. O. Wilkes, "Applied Numerical Methods," John Wiley, N.Y., p. 451 (1969).

Castro, J. M., and C. W. Macosko, "Studies of mold filling and curing in the reaction injection molding process," *AIChE J.*, **28**, 250 (1982).

Denbigh, K., "Chemical reactor theory, an introduction," Cambridge University Press, p. 57 (1965).

Domine, J. D., and C. G. Gogos, "Simulation of reactive injection molding," *Polym. Eng. Sci.*, **20**, 13, 843 (1980).

Kamal, M. R., and S. Kenig, "Injection Molding of Thermoplastics," *Polym. Eng. Sci.*, **12**, 294 (1972); **12**, 302 (1972).

Kamal, M. R., and M. E. Ryan, "The behavior of thermosetting compounds in injection molding cavities," *Polym. Eng. Sci.*, **20**, 13, 859 (1980).

Lee, L. J., "Polyurethane reaction injection molding: process, materials, and properties," *Rubber Chem. Tech.*, **53**, 3, 542 (1980).

Lipshitz, S. D., "Laminar Tube Flow with a Thermosetting Urethane Polymerization," Ph.D. Thesis, University of Minnesota (Feb., 1976).

Lipshitz, S. D., and C. W. Macosko, "Rheological changes in a urethane network polymerization," *Polym. Eng. and Sci.*, **16**, 803 (1976).

Lipshitz, S. D., and C. W. Macosko, "Kinetics and energetics of a fast polyurethane cure," *J. Appl. Polym. Sci.*, **21**, 2029 (1977).

Lord, H. A., and G. Williams, "Mold filling studies for the injection molding of thermoplastic materials," *Polym. Eng. Sci.*, **15**, 553 (1975); **15**, 569 (1975).

Lynn, S., and J. E. Huff, "Polymerization in a tubular reactor," *AIChE J.*, **17**, 475 (1971).

McAdams, W. H., "Heat Transmission," McGraw-Hill, 3rd ed., p. 322 (1954).

Prepelka, P. J., and J. L. Wharton, "Reaction injection molding in the automotive industry," *J. Cellular Plastics*, **11**, 87 (1975).

Richter, E. B., and C. W. Macosko, "Kinetics of fast (RIM) urethane polymerization," *Polym. Eng. Sci.*, **18**, 1012 (1978).

Sala, R., F. Valz-Grez, and L. Zanderighi, "A fluid dynamic study of a continuous polymerization reactor," *Chem. Eng. Sci.*, **29**, 2205 (1974).

Tadmor, Z., E. Broyer, and C. Gutfinger, "Flow analysis network: a method for solving flow problems in polymer processing," *Polym. Eng. Sci.*, **14**, 660 (1975).

Tadmor, Z., and I. Klein, "Engineering principles of plasticating extrusion," *Pol. Eng. and Sci.*, **14**, 122 (1974).

Tadmor, Z., and C. G. Gogos, "Principles of polymer processing," John Wiley and Sons, New York (1979).

Van Krevelan, D. W., "Properties of polymers," Elsevier, Amsterdam (1972).

Wallis, J. P. A., R. A. Ritter, and H. Andre, "Continuous production of polystyrene in a tubular reactor," *AIChE J.*, **21**, 686 (1975); **21**, 691 (1975).

Manuscript received March 31, 1978; revision received January 27, and accepted January 28, 1982.

Optimum Dimensions for Pipeline Mixing at a *T*-Junction

Conditions are identified which insure optimum pipeline mixing at a *T*-junction. Analytical expressions, that result from detailed measurements of both near and far-field momentum-dominated jet trajectories in a crossflow, are renormalized in terms of pipe coordinates. It is demonstrated that a simple scaling law exists for the limiting geometry of either large or small jet-to-pipe diameter ratios. The scaling laws are shown to accurately correlate existing data for each limiting geometry.

L. J. FORNEY and H. C. LEE

School of Chemical Engineering
Georgia Institute of Technology
Atlanta, GA 30332

SCOPE

Turbulence promotes most important chemical reactions, heat transfer operations and mixing and combustion processes in industry. Effective use of turbulence increases reactant contact and decreases reaction times which can significantly reduce the cost of producing many chemicals. It is common in existing chemical process units to mix two fluids at a tee in a pipe with subsequent transport to other locations. For numerous continuous pipeline mixing applications, the feed jets are directed perpendicular to the pipe axis. The distance necessary to achieve a desired degree of uniformity of concentration or temperature in the pipe depends on the following quantities: ratio of jet-to-pipe diameter, uniformity criterion, ratio of jet-to-pipe velocity, ratio of specific gravities of the two feed streams and the pipe or jet Reynolds number and surface roughness. Simpson (1975) and Gray (1982) have prepared reviews of pipe mixing with tees and other geometries.

Chilton and Genereaux (1930) recorded the pioneering, although elementary, experimental results for optimum mixing with a *T*-junction. Most of the existing data were taken by Forney and Kwon (1979) using improved quantitative techniques for a range of diameter ratios $0.025 \leq d/D \leq 0.2$. Forney and Kwon also developed an expression to predict optimum dimensions for a side-tee mixer by assuming that optimum mixing conditions were achieved if the jet and pipe axis coincided at a fixed distance from the point of injection. Although the constraint of geometric similarity imposed on their near-field jet trajectories within a pipe provided useful results, the slope of their theory was imperfect compared with existing data for large diameter ratios $d/D > 0.035$. Moreover, the form of

0001-1541-82-6469-0980-$2.00.